Subfemtosecond soft-x-ray generation from a two-level atom: Extreme carrier-wave Rabi flopping

S. Hughes*
Department of Physics, University of Surrey, Guildford, Surrey GU2 7XH, Great Britain
(Received 01 May 2000; published 13 October 2000)

We report a different mechanism to generate x-ray transients by exploiting high-field nonperturbative subcarrier-wave coherent phenomena. The interaction of several-cycle optical pulses with a nonlinear material results in carrier-wave Rabi flopping that acts as an alternative source for x-ray generation.

PACS number(s): 42.50.Hz, 42.50.Md, 42.50.Gy, 42.65.−k

The interaction of intense fields with nonlinear materials has recently entered the *extreme* regime. This new area of nonlinear optics is partly due to tremendous developments in ultrashort and ultra-intense lasers, and partly due to new theoretical predictions and innovative experimental techniques used to explore nonperturbative quantum mechanics in real time. When a laser-pulse duration approaches the optical period, a qualitatively different regime of strong-field laser-material interactions is entered: *extreme nonlinear optics* [1]. New behavior results as a consequence of the quasisingle-cycle excitation and the fact that the electric field rather than the intensity envelope governs the interaction, which is typical of a nonperturbative regime.

For example, the process of high-harmonic generation (HHG) due to an intense atom-field interaction has received a great deal of attention in recent years [2,3], and coherent short-wavelength radiation well into the x-ray region has been demonstrated. Moreover, harmonically generated x-ray transients as short as 100 asec have been predicted [4]. The observed spectrum of harmonics is affected by both the single-atom emission and the ensuing collective behavior. In layman's terms, the generation of high harmonics of a laser irradiating an ensemble of atoms can be viewed as follows: each atom emits radiation that propagates in the remaining atoms, ions, and ionized electrons; consequently, they interfere, scatter, and may stimulate further harmonic emission. The theoretical problem of HHG is most fruitfully treated nonperturbatively in the atom-field interaction and is a fascinating problem. For Rydberg atoms [5], higher frequency harmonics are produced from continuum- to bound-state transitions, in which electrons release the energy absorbed from the field during its excursion in the continuum. The harmonic generation in atoms presents extensive plateaus [6] (an extensive region of similar spectral intensity in frequency extending well above the fundamental excitonic binding energy). High intensity femtosecond laser-induced plasmas in metal-doped targets are also being actively studied for applications of x-rays generated from Ti:sapphire laser pulses with intensities in excess of 10^{15} W/cm^2 [7]. Short-pulse x-rays will enable the creation of innovative methods for optoelectronics and materials research in unprecedentedly short time and space scales. X-ray fields are also of great importance for biological microscopy and semiconductor lithography.

One consequence of these new several-cycle laser systems is that some of the old theoretical tools do not provide an adequate description. Besides a few examples [8–15], one usually begins by employing the appropriate coupled matter-Maxwell equations within the slowly varying envelope approximation (SVEA), i.e., the envelopes of the electromagnetic field and polarization are assumed to vary little over an optical period and wavelength. Recently we have demonstrated that even the familiar process of Rabi flopping [16] can change significantly [17]. When a resonant excitation field drives the excitation from the ground state to the excited state and back again, this is termed Rabi flopping (RF) [18–20]. The usual analysis of RF assumes that the optical-frequency components of the energy density do not contribute to the nonlinearity; however, several different features arise in the full Maxwell solution that are absent in the standard SVEA models. It was shown that the nonlinear behavior is dependent not only on the electric-field envelope, but also on its propagating time-derivative effects. Standard SIT 2π and 4π pulses are essentially reproduced with minor modifications due to local carrier effects in agreement with Ref. [11]. However, for higher pulse areas, it is found that carrier-wave effects become predominant, and a different type of carrier-wave Rabi flopping (CWRF) occurs. The current effort exploits this phenomenon to demonstrate that realistic optical pulses interacting with a two-level atom (TLA) should lead to the generation of x-ray transients. This alterative prediction is a direct manifestation of CWRF.

We model pulse propagation of various $2l\pi$ optical pulses (where l is an integer) of 18 fs time duration (full width at half maximum irradiance). As highlighted above, for pulse areas (the integral of its Rabi frequency over time) of $2l\pi$, the standard results for $l>2$ do not hold because of a strong reshaping of the individual optical carriers [17]. Therefore the electric-field time-derivative effects will lead to CWRF, and, subsequently, to the formation of higher spectral components on the propagating pulse. The propagation distances required to induce strong carrier reshaping are determined by the TLA-material parameters.

Turning now to a tractable model, we employ a standard finite-difference time-domain [FDTD] [11,12,21] approach for solving the full-wave Maxwell equations, and a fourth-order Runge-Kutta method to solve the Bloch equations. Further details are given in Ref. [17]. Basically, we solve for the nonlinear polarization $P_{\rm nl}=2Nd\,{\rm Re}[\rho_{12}]$, where N is the

*Email address: steve.hughes@surrey.ac.uk

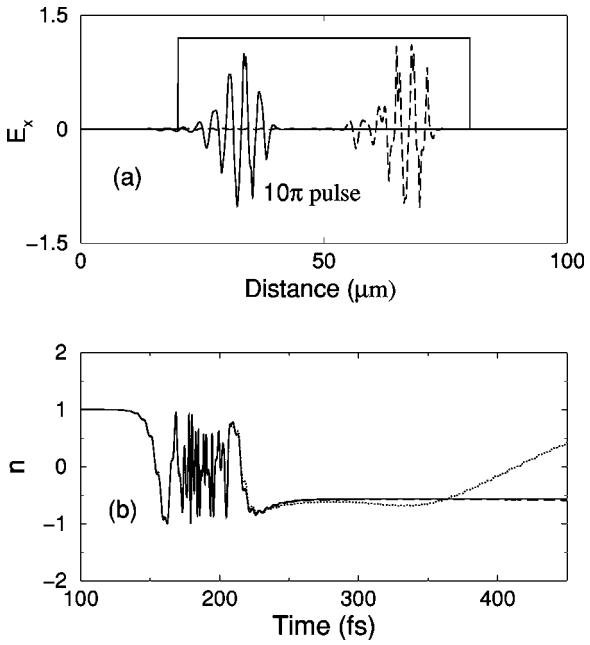

FIG. 1. (a) 10π-pulse propagation through the two-level system (thick solid curve). The normalized field is shown at the respective times of 350 fs (solid curve) and 460 fs (dotted curve). (b) Inversion n (solid curve) near the front face of the two-level material ($z=21$ μm). The dashed and dotted curves correspond to simulations with a larger dipole moment (see text).

density of TLA's, and ρ_{12} is the off-diagonal density-matrix element obtained from the optical Bloch equations. The initial field $E_x(z=0,t)=\hat{\mathbf{n}}_x E_0 \mathrm{sech}[-(t-\tau_{\mathrm{off}}/\tau_0)]\sin(\omega t)$, where E_0 is the peak input electric field, τ_{off} is the offset position of the pulse center (at t=0), $\tau_p=2\ \mathrm{arcosh}(1/\sqrt{0.5})\tau_0$ is the full width at half maximum (FWHM) of the pulse irradiance profile, $\hat{\mathbf{n}}_x$ is a unit vector perpendicular to the direction of propagation, and $\omega=2\pi c/\lambda_0$ is the central pulse frequency. Within the SVEA, it is well established that when the envelope of the pulse has an area that is an integer number of 2π, then lossless propagation is possible. For a $2l\pi$ pulse, the rotating dipoles are exactly returned to their initial state while maintaining the shape of the excitation pulse while exhibiting l Rabi flopps. This will occur when $E_0^{2l\pi}=2l\hbar/d\tau_0$. The carrier frequency $\omega=\omega_{12}=0.6\times10^{15}\mathrm{rads}^{-1}$, $\tau_p=18$ fs, and $d=2.65$ eÅ. All other material and laser parameters are identical to those in Ref. [17].

The peak amplitude of the necessary pulse to achieve a 10π envelope area is approximately 2.5 GV/m. (This corresponds to an irradiance of $\approx 8\times10^{13}\,\mathrm{W/cm^2}$ in vacuum.) Figure 1(a) shows an example of a propagating 10π pulse through the TLA medium. The pulse initially propagates in the free-space region, and thereafter enters the two-level medium at 20 μm; the pulse then propagates the nonlinear medium and exhibits strong reshaping (dotted curve). Importantly, the shaping takes place for the individual cycles rather than the envelope of the pulse itself; this carrier reshaping is caused by subcarrier Rabi flopping, which can be seen in Fig. 1(b). Even at these optical fields—an area of 10π (which is modest by today's laser standards)—nonlinear carrier-wave effects can be clearly observed during pulse propagation. This leads to the formation of a subpulse at later times. Note that this effect is due to a breakdown in the slowly varying envelope approximation in time and not in space (see below). The 10π-pulse simulation does not recover well known, SVEA (analytic or otherwise) results in agreement with Ref. [17]. For comparison, Fig. 1(b) shows the corresponding temporal development of the inversion n (solid curve) at the fixed position of $z=21$ μm that is near the input surface of the nonlinear medium. Oscillation features at the zero points of the pulse arise due to the time-derivative behavior of the input field (see also Ref. [11]). We note that incomplete Rabi flops occur instead of the anticipated integer number. Maxwell's curl equations also account for backwards propagating fields, which do not occur in the present study since the linear refractive index is unity, and also because the absorption length is too large (thus the SVEA in space is valid here). To demonstrate this we have performed additional calculations by increasing the dipole moment (thus decreasing the absorption length) by a factor of 10 and 100 shown, respectively, by the dashed and dotted curves. The input pulse areas are kept fixed. The former case is almost identical to the previous calculations, while the latter results do indeed display strong back propagation effects. Unusual back propagation effects will be discussed in future work. For the present study the SVEA in space holds.

We now probe even deeper into this effect and show that (i) CWRF still occurs when the carrier frequency is increased to $\omega=\omega_{12}=2\times10^{15}\,\mathrm{rads}^{-1}$, where one might expect the SVEA in time to work. (ii) The propagating pulse will contain *extremely* higher frequency components that show some similarities with those produced via HHG. Furthermore, this later result can now be controlled somewhat via the chosen area of the input pulse. We continue with the original dipole parameters but now increase the carrier frequency to the above value which, to the eye (see Fig. 2) and intuition, looks like it should certainly satisfy the RWA. It does not. We demonstrate that even an area of only 20π is sufficient to cause strong carrier-wave nonlinear effects that cannot be modeled by employing the SVEA equations. In Figs. 2(a) and 2(b) we show, respectively, the density changes and the corresponding electric field near the input face of the TLA. To help clarify the physics we also show an enlargement of the carrier-wave effects at around 150–160 fs, shown in Figs. 2(c) and 2(d). Propagation effects are highlighted below.

It is evident that CWRF induces carrier-wave reshaping so we now look at propagation effects for a 20π and 200π pulse. As a possible experimental probe one can monitor the output spectrum of the propagated pulse. Figures 3(a) and 3(b) show, in comparison to the input spectrum, the output irradiance of 20π and 200π pulses. The top curve [Fig. 3(a)] clearly shows that even with an input central frequency of $\approx$1.3 eV, there is the appearance of a plateau and eventually a cutoff after about 20 eV. Additionally, these features recall some similarities with HHG in high-field atomic physics, though now we are working with an initially resonant

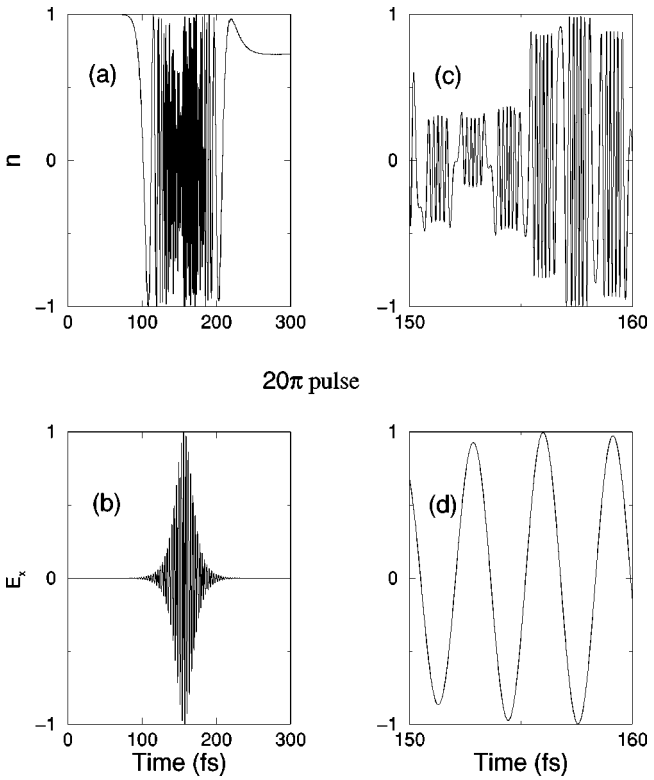

FIG. 2. (a) As in Fig. 1(b) but for 20π-pulse propagation with a greater carrier frequency and resonant frequency (see text). (b) Corresponding electric field vs time. (c) Enlargement of Fig. 2(a) around 150–160 fs. (d) Enlargement of Fig. 2(b) around 150–160 fs.

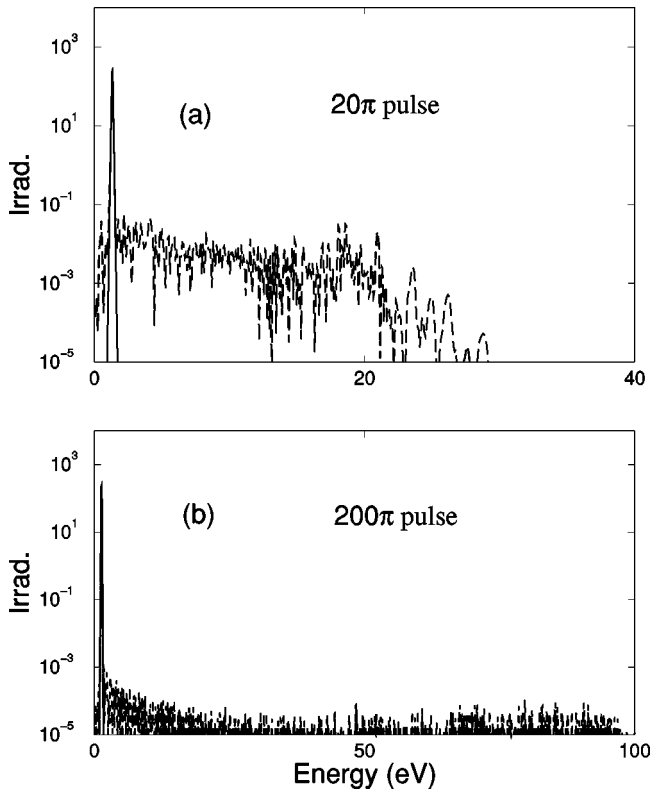

FIG. 3. (a) Input (solid curve) and output (dotted curve) pulse irradiance spectra for 20π-pulse propagation. (b) As in Fig. 3(a) but for 200π-pulse propagation.

nonlinearity. The results for the 200π pulse are even more intriguing: one now discerns frequency components up to100eV and clearly transients well into the x-ray regime can be generated. At this point we must correctly point out that the TLA is only an approximate model at this stage since it will now, for example, include higher states that may absorb the higher frequency components; our present purpose is to bring to the forefront the basic new physics for a strict TLA. A proper experimental prediction would have to pay more attention to the exact material under investigation. Second, we stress that these transients are not numerical artifacts; for the simulations we choose $50l$ (i.e., 10 000 for the latter simulation) points per wavelength and have checked that the results are identical for much smaller space and time steps. For the experimentalists in the field, we suggest a multiple-π pulse propagation study to monitor the higher frequency components of the transmitted pulse. In any case, our simulations show that extraneous features will be evident that are not captured within the slowly varying envelope models and such techniques may also form a basis for the generation of x-ray transients.

In conclusion, we have obtained interesting suboptical-carrier transient effects that may form a basis for generating x-ray transients nonperturbatively. This different ultrafast phenomenon is demonstrated by solving Maxwell's curl equations coupled to a two-level atom without invoking any slowly varying envelope approximations. Under such extreme conditions a more accurate model may be required for describing matter with multiple energy levels. Nevertheless, this model is exact insofar as the full Maxwell equations and two-level atomic model are exact. The induced spectrum of the propagating pulse contains a range of frequency components that resemble some similar characteristics to high-harmonic generation in atoms, though via a completely different mechanism. It remains to be seen whether such effects will occur in real atoms where bound-bound transitions and ionization become important, however, the results for the simplified model are sufficiently encouraging to tempt experimental investigation.

[1] See, for example, F. Krausz *et al.*, Opt. Photonics News **9** (7), 46 (1998).

[2] M. Protopapus, D.G. Lappas, and P.L. Knight, Phys. Rev. Lett. **79**, 4550 (1997); G.G. Paulus *et al. ibid.* **80**, 484 (1998).

[3] J. Zhou *et al.*, Phys. Rev. Lett. **76**, 752 (1996).

[4] I.P. Christov, M.M. Murnane, and H.C. Kapteyn, Phys. Rev. Lett. **78**, 1251 (1997).

[5] J.L. Krause *et al.*, Phys. Rev. Lett. **79**, 4978 (1998).

[6] P. Moreno, L. Plaja, and L. Roso, J. Opt. Soc. Am. B **13**, 430 (1996).
[7] See, for example, T. Nishikawa *et al.*, Appl. Phys. Lett. **13**, 1653 (1997); H. Nakano *et al.*, *ibid.* **69**, 2992 (1996).
[8] S. Swain, J. Phys. A **6**, 192 (1973).
[9] J. Bromage *et al.*, Opt. Lett. **22**, 627 (1997).
[10] A. Schülzgen *et al.*, Phys. Status Solidi B **206**, 125 (1998).
[11] R.W. Ziolkowski *et al.*, Phys. Rev. A **52**, 3082 (1995).
[12] S.A. Basinger and D.J. Brady, J. Opt. Soc. Am. B **11**, 1504 (1994).
[13] W. Forysiak *et al.*, Phys. Rev. Lett. **76**, 3695 (1996).
[14] R.G. Flesch *et al.*, Phys. Rev. Lett. **76**, 2488 (1996).
[15] T. Brabec and F. Krausz, Phys. Rev. Lett. **78**, 3282 (1997).
[16] L. Allen and J. H. Eberly, *Optical Resonance and Two-Level Atoms* (Wiley, New York, 1995).
[17] S. Hughes, Phys. Rev. Lett. **81**, 3363 (1998).
[18] I.I. Rabi, Phys. Rev. **51**, 652 (1937).
[19] I.I. Rabi *et al.*, Phys. Rev. **53**, 318 (1938).
[20] S.L. McCall and E.L. Hahn, Phys. Rev. Lett. **18**, 908 (1967); G.L. Lamb, Jr., Rev. Mod. Phys. **43**, 99 (1971).
[21] D.M. Sullivan, IEEE Trans. Microwave Theory Tech. **43**, 676 (1995).